Multiplexing Schemes for sub-THz/THz Interconnects (Invited)

Xuan Ding, Bo Yu, Hai Yu, Sajjad S. Saber and Qun Jane Gu
Department of Electric and Computer Engineering
University of California Davis, Davis, CA 95616, USA
Email: xxding@ucdavis.edu and jgu@ucdavis.edu

***Abstract*—This paper discusses the multiplexing schemes for sub-THz/THz Interconnect, which has the potential to complement the existing electrical and optical interconnects. Using a wideband and low-loss Si dielectric waveguide (DWG) as the medium, the proposed sub-THz/THz interconnect achieves tens of Gbps date rates with high energy-efficiency with the potential to reach a longer distance than electrical interconnects. The bandwidth density can be further boosted by employing advanced multiplexing schemes. Frequency division, mode division and polarization multiplexing are discussed and demonstrated. The simulated and measured results show that the multiplexing schemes expand the transmission bandwidth by introducing multiple sub-channels with crosstalk < -20 dB.**

Keywords—Multiplexing, sub-THz/THz, interconnect, frequency division, polarization, multi-mode.

I. Introduction

According to the Shannon Theorem, channel bandwidth and attenuation constant, which determine SNR, are the key factors to determine communication systems' data capacities. Two existing interconnects are facing their bottlenecks: Electrical interconnect suffers from the limited bandwidth and quickly increasing losses over distance and bandwidth; Optical fiber has ultra-wide bandwidth and low insertion loss, but optic links need high-power laser sources and complex fabrication and packaging, which constrain its applications. High-resistivity Si ($\varepsilon_r = 11.9$, $\tan\delta = 0.001$ [1]) DWG based sub-THz/THz interconnect demonstrates high potential to address the long-standing challenge to satisfy ever-increasing data rate and energy efficiency requirements by leveraging the advantages of electrical and optical interconnects, especially in the most challenging meter-range scenario [2].

Si DWG demonstrated 3-dB bandwidth of 59 GHz and transmission loss (TL) better than 4 dB [3]. To take fully advantage of the bandwidth, it is beneficial to adopt multiplexing schemes to split one physical channel into several sub-channels logically, to relieve the system and active circuits specification requirements, such as the dispersion of DWG and bandwidth of transmitter and receiver, thus boost the total data rate. There are five dimensions of multiplexing: time, frequency, mode, polarization and quadrature [4]. Time multiplexing does not increase the throughput. Quadrature multiplexing requires advanced signal processing and high order modulations, thus increasing performance requirements of system building blocks, such as PLL, ADC, DAC and clock distribution. As a subsequence, it may not be very energy efficient and is not the focus of the sub-THz/THz interconnect.

This paper is organized as follows. In Section II, frequency division, mode division and polarization multiplexers at sub-THz are investigated, designed, and demonstrated, respectively. The results of each structure exhibit good agreements between simulation and measurement results. The fabrication process and measurement setup is introduced in Section III, and the conclusion is presented in Section IV.

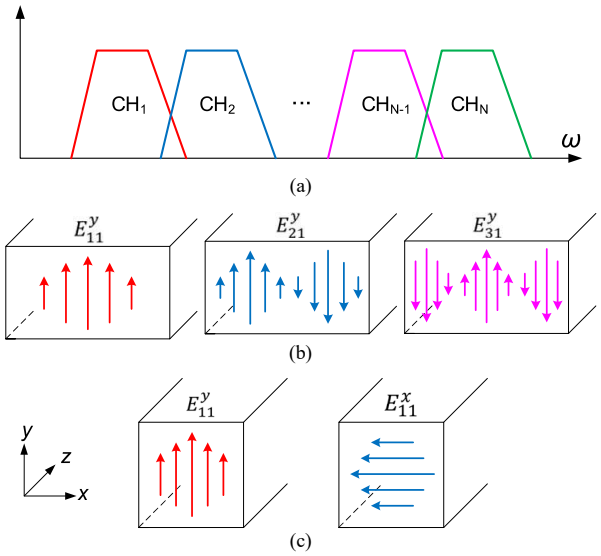

Fig. 1. (a) Frequency division, (b) mode division, and (c) polarization multiplexing.

II. Multiplexing Schemes at sub-THz/THz

The circuit design and fabrication at sub-THz/THz are challenging because the smaller feature dimensions require high precision in modeling and fabrication. Three multiplexing schemes based on frequency division [5], mode division and polarization [6], are investigated and demonstrated. The mechanism is shown in Fig. 1.

A. Frequency Division Multiplexing

Frequency division multiplexing is combining and transmitting multiple communication signals in parallel at distinct carrier frequencies over the same transmission medium, as shown in Fig. 1 (a). Each sub-channel is required to have enough bandwidth to support high data rate and sufficient out-of-band suppression to reduce crosstalk interference. Planar bandpass filter (BPF) is a good candidate of frequency division multiplexer. High quality factor (Q) substrate is preferred to realize the channel selection filter, which can minimize the TL and improve the suppression by cascading more stages.

To illustrate frequency division multiplexing, a dual-band sub-THz channel is designed, as shown in Fig. 2 (a), which consists of Si DWG, microstrip line (MSL)-to-DWG transition and a pair of diplexers. MSL-to-DWG transition in Fig. 2 (b) smoothly transfers quasi-TEM mode in MSL to E_{11}^y

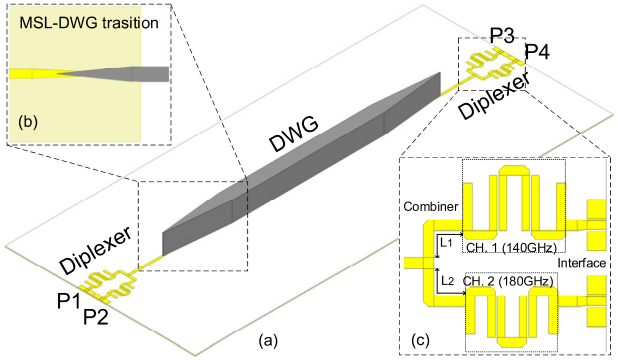

Fig. 2. (a) Stucture of the dual-band channel, (b) MSL-to-DWG transition, and (c) diplexer on BCB substrate.

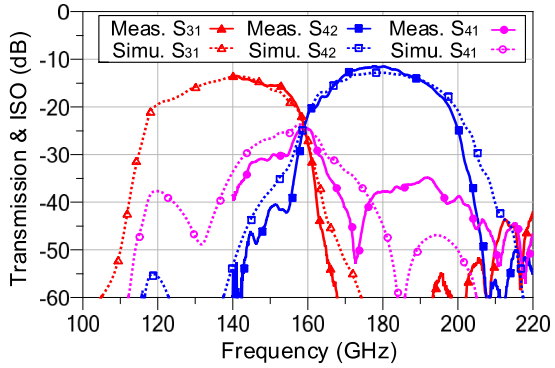

Fig. 3. Simulated and measured S-parameters of the dual-band channel.

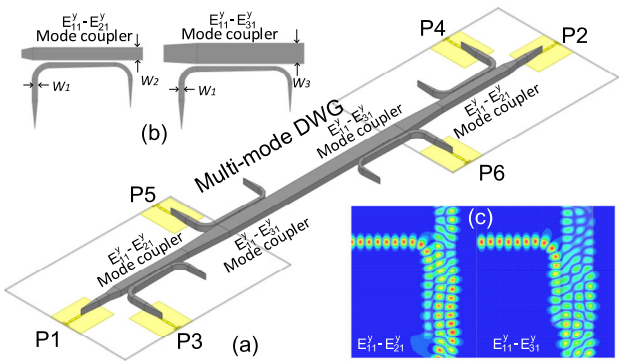

Fig. 4. (a) Stucture of the multi-drop channel, (b) mode coupler between $E_{11}^{y} - E_{21}^{y}$ and $E_{11}^{y} - E_{31}^{y}$, and (c) their E field distrubution.

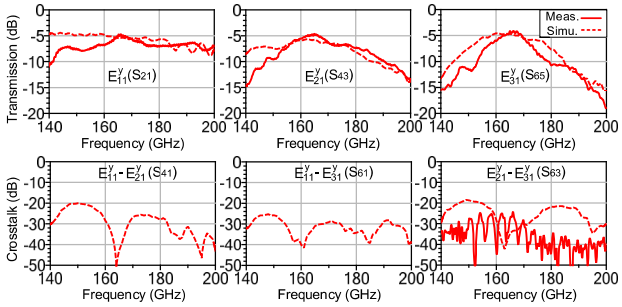

Fig. 5. Simulated and measured S-parameters of the multi-drop channel.

mode in DWG for a wide frequency band. The diplexer, as the only bandpass component in the channel, determines the frequency selection performance and is synthesized on dielectric substrate of 20-μm BCB. Its $\varepsilon_r = 2.9$ and $\tan\delta = 0.03$ are calibrated at 165 GHz, which is necessary for frequency sensitive components above mm-Wave. The sub-THz diplexer, as illustrated in Fig. 2 (c), is constructed with BPFs, a combiner and ground-signal-ground (GSG) interface. Conventional hairpin BPF adopting edge-coupled resonators has the compact size due to folded λ/2 MSL approaches. The center frequencies of the BPFs in the diplexer are 140 and 180 GHz, respectively, and the bandwidth is more than 20 GHz to support high data-rate communications. The simulated insertion loss is about 3 dB and suppression in the adjacent bands is more than 20 dB. When the two BPFs are combined, one BPF will be part of the loading to the other BPF. To minimize the loading effect, 50-ohm L_1 and L_2, which have minor effect in its passband but significant effect on the adjacent band (the passband of the other BPF), are tuned to present a high-impedance to the other BPF.

The simulated and measured S-parameters of the dual-band sub-THz channel are plotted in Fig. 3. The measured TL for CH. 1 (140 GHz) S_{31} and CH. 2 (180 GHz) S_{31} archives the minimum value of 13.2 dB within 3-dB bandwidth of 127.7-152.3 GHz and 11.7 dB within 3-dB bandwidth of 168.3-191.0 GHz, respectively. The measured isolation is more than 30 dB, which is sufficient to suppress crosstalk.

B. Mode Division Multiplexing

Si DWG allows multiple modes existing simultaneously and different modes are naturally isolated from each other. Taking advantage of this feature can transmit data over different sub-channels in a same physical link. Fig. 1 (b) shows a multi-mode channel with isolated E_{11}^{y}, E_{21}^{y} and E_{31}^{y} modes. Mode converters transfer modes and combine signal streams. The challenge of this design lies in maximizing the coupling efficiency to a desired mode and avoiding stimulating other unwanted modes and crosstalk interference.

Fig. 4 (a) illuminates a multi-drop channel that consists of a multi-mode Si DWG, MSL-to-DWG transition and mode couplers implementing mode conversion between E_{11}^{y} and E_{21}^{y}, E_{11}^{y} and E_{31}^{y}, respectively. The coupling always exists when the unshielded DWGs approach close, and it happens between the same modes (for example E_{11}^{y} and E_{11}^{y}) or different modes (such as E_{11}^{y} and E_{21}^{y}). The condition for mode coupling are field overlap and phase matching. Field overlap means DWGs are close enough and field in each waveguide is interacting. Phase matching requires that the propagation constant β, which is the wavenumber along propagation direction, are equal for those modes. By precisely controlling the width of DWG, the effective refractive index n_{eff} of a specific mode can be finely tuned, then it is possible to make two modes phase matched.

$$\beta = n_{eff} \cdot \frac{\omega}{c}$$

where ω angular frequency and c is the speed of light in vacuum. As shown in Fig. 4 (b), mode E_{11}^{y} is fed from the branch DWG with W_1=300 μm, which has the same n_{eff} of E_{21}^{y} in a DWG with W_2=760 μm and E_{31}^{y} in a DWG with W_3=1200 μm, then coupling happens between E_{11}^{y} and E_{21}^{y}, E_{11}^{y} and E_{31}^{y}, as shown in Fig. 4 (c).

The simulated and measured S-parameters of the multi-drop channel are plotted in Fig. 5. The minimum measured TL

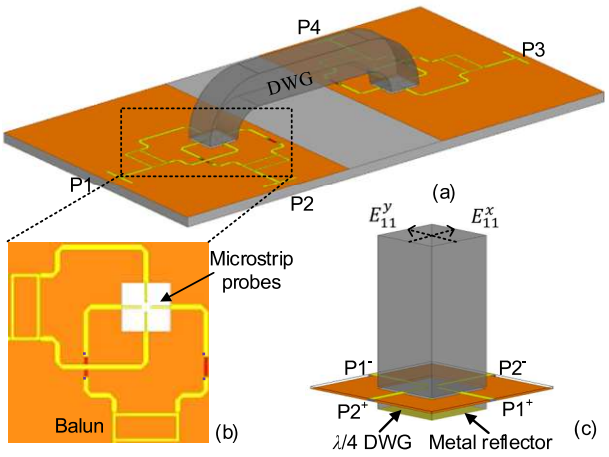

Fig. 6. (a) Stucture of the ortho-mode channel, (b) single-ended to differential transition, and (c) probe-based MSL-to-DWG trasition.

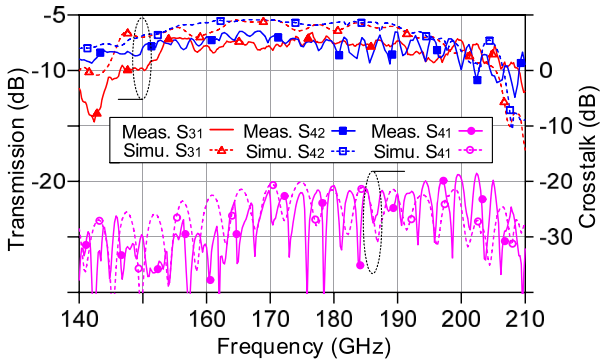

Fig. 7 . Simulated and measured S-parameters of the ortho-mode channel.

for E_{11}^{y} , E_{21}^{y} and E_{31}^{y} are 5 dB within the 3-dB bandwidth of 143-200 GHz, 151-185 GHz and 155-174 GHz, respectively. Due to the constrain of measurement setup, the only measured crosstalk between E_{21}^{y} and E_{31}^{y} mode is better than -25 dB.

C. *Polarization multiplexing (Orthogonal mode)*

Polarization multiplexing also can realize simultaneous transmission of multiple information streams. The orthogonal modes, E_{11}^{x} and E_{11}^{y} in Fig. 1 (c), are transferred by a polarization diplexer, which is a device combining or separating orthogonally polarized signals. The orthogonal modes are intrinsically isolated because of the polarization.

Fig. 6 (a) shows the ortho-mode DWG channel. There are two orthogonal fundamental modes, E_{11}^{x} and E_{11}^{y}, supporting the signal propagations via the P1-to-P3 path (S_{31}) and the P2-to-P4 path (S_{42}), respectively. It consists of a pair of single-end to differential baluns in Fig. 6 (b), probes-based MSL-to-DWG transition in Fig. 6 (c) and an isotropic rectangular DWG. The differential probes-based MSL-to-DWG transition is proposed to form a differential mode intrinsically to excite E_{11}^{x} or E_{11}^{y} mode in the DWG. The identical pair of microstrip probes are fed with differential EM waves, and a reflector is placed λ/4 away from the feeding position, provides out-of-phase signal cancellation and only allows the EM waves propagate along the up direction of the DWG. The balun was optimized and achieved less than 1.5 dB magnitude mismatch and 7° phase mismatch at the range of 140-190 GHz. To implement a planar interconnect, the DWG is bended, but introduce the asymmetric bending issue and large ripples occurs for an ortho-mode DWG if the bending radius is less 1000 μm at 165 GHz.

The TL for E_{11}^{y} and the mode E_{11}^{x} are 6.6 dB from 151.1 to 171.4 GHz and 6.5 dB from 150.8 to 206 GHz, respectively. The crosstalk between orthogonal mode is better than -20 dB in the range of 140-210 GHz.

III. Fabrication and Measuremnts Setup

The entire structure was modelled in full-wave simulator HFSS and measured on-wafer with G-band (140 to 220 GHz) S-parameters testbench. All parts are fabricated in-house with micro-manufacturing process. The Si DWG is produced by deep reactive ion etching (DRIE). MSL-to-DWG transitions and diplexer are fabricated using lithography on a thin-film substrate BCB or quartz, and then assembled with the Si DWGs by a flip-chip bonder to form the channel structures. All the structures are connected with 100-μm pitch GSG pads, so they can be test with commercial probes.

The measurement setup with an Agilent network analyzer (PNA-X N5247A), a pair of Virginia Diodes frequency extension modules (VDI WR5.1-VNAX), WR-5 (140-220 GHz) S-bend waveguides, and a pair of WR-5 probes. The SOLT (Short, Open, Load, Thru) calibration method is employed to set the reference plane at the probe tip.

IV. Conclusion

Three different multiplexers, which are in frequency division, mode division and polarization domains, are introduced and demonstrated in this paper. All of them achieve good transmission and isolation performance that can satisfy the high-speed chip-to-chip communications. The mode multiplexer can dramatically boost the data rate and bandwidth density of a sub-THz/THz interconnect, and are able to connect transceivers at different places, which works like a data bus. A smooth mode transition is a key factor to determine the overall performance of a mode multiplexing system.

Acknowledgment

The authors would like to acknowledge National Science Foundation (NSF) for partial funding support and the UC Davis Center for Nano and Micro Manufacturing (CNM2) for the fabrication.

References

[1] B. Yu et al., "Sub-THz interconnect for planar chip-to-chip communications," in IEEE 18th Topical Meeting on Silicon Monolithic Integrated Circuits in RF Systems (SiRF), 2018, pp. 54-56.

[2] Q. J. Gu, "Sub-THz/THz Interconnect, Complement to Electrical and Optical Interconnects: Addressing Fundamental Challenges Related to Communication Distances," *IEEE Solid-State Circuits Mag.*, vol. 12, no. 4, pp. 20-32, Fall 2020.

[3] Q. J. Gu *et al*., "THz interconnect for inter-/intra-chip communication," in *SPIE Defence + Commercial Sensing*, April, 2019.

[4] P. Winzer, "Making spatial multiplexing a reality," *Nature Photon 8*, 345–348, 2014.

[5] X. Ding, *et al*., "An FDD-based Full-Duplex Sub-THz Interconnect with Data-rate of 22.6 Gb/s and Energy-Efficiency of 1.58pJ/bit," in *2021 46th International Conference on Infrared, Millimeter and Terahertz Waves (IRMMW-THz)*, 2021, pp. 2021–2022.

[6] B. Yu *et al.*, "Ortho-Mode Sub-THz Interconnect Channel for Planar Chip-to-Chip Communications," *IEEE Trans. Microw. Theory Tech.*, vol. 66, no. 4, pp. 1864–1873, 2018.